Design and Potential Applications of Floating Structures in Singapore

Kok Keng Ang, Jian Dai, Oyvind Hellan, Arnstein Watn and Michael Boon Ing Si

Abstract As an island city-state with about 710 km^2 of land, Singapore treats land as a precious and limited resource. In order to sustain the development growth, Singapore continues to reclaim land from the sea and excavate underground space. In addition, Singapore has also started creating space on the sea by using large floating structure technology. This paper focuses on a multi-purpose floating structure (MPFS) research and development project funded by Land and Liveability National Innovation Challenge (L2 NIC) Directorate and JTC Corporation. The objective of the project is to develop innovative design concepts, optimal structural, and foundation solutions, as well as construction and installation methods for multi-purpose floating structures in Singapore coastal waters. This paper covers three specific applications, namely a floating hydrocarbon storage facility, a floating bridge and a modular multi-purpose floating structure. The technical challenges, conceptual designs, research innovation and key findings will be discussed. The outcomes of this research project may be used as a reference for other potential applications including floating offshore bunker supply bases, LNG regasification facilities, solar plants, desalination plants, piers, shipyards, container port terminals, golf courses, parks and towns/cities.

Keywords Large floating structure · Modular floating structure · Hydrocarbon storage facility · Floating bridge

1 Introduction

As an island city-state with about 710 km^2 of land, Singapore treats land as a precious and limited resource. In order to sustain the development growth, Singapore continues to reclaim land from the sea.

K. K. Ang (✉) · J. Dai · M. B. I. Si
Department of Civil & Environmental Engineering, National University of Singapore, Singapore 117576, Singapore
e-mail: ceeangkk@nus.edu.sg

O. Hellan · A. Watn
SINTEF Ocean, Trondheim, Norway

Besides land reclamation, the large floating structure (VLFS) technology is one of the approaches that Singapore is using in creating space on the sea. Building large floating structures is feasible because of Singapore's benign sea state condition and strong offshore construction capability. Towards exploring and implementing large floating structure applications, the Land and Liveability National Innovation Challenge (L2 NIC) Directorate and JTC Corporation have provided S$7.13 million in research grant to the National University of Singapore (NUS) and SINTEF to conduct research on multi-purpose floating structures (MPFS). The objective of the MPFS research and development project is to develop design concepts, innovative and optimal structural, foundation and construction solutions for large floating structures. The project focuses on three specific applications, namely the floating hydrocarbon storage facility (FHSF), the floating bridge (FB) and the modular multi-purpose floating structure (MMFS).

The study on the FHSF focuses on the development of the world's first floating prestressed concrete facility that can accommodate 300,000 m^3 stockpile of hydrocarbon products. The research tasks include evaluation of existing design concepts, development of innovative design concepts, detailed structural and hydrodynamic analyses, providing innovative foundation, material and construction solutions as well as design and conduct of physical model tests.

Similarly, the study on the FB focuses on the evaluation of existing floating bridges and development of innovative design concept and solution of a floating bridge spanning over 500 m of waterbody. Structural and hydrodynamic performances of the proposed floating bridge concept have been investigated. The objective of this research aims to develop a novel and cost-effective design concept for ASEAN's first floating bridge.

The objective of the track on MMFS is to develop innovative solutions for the creation of 'land on sea' of any desired size and shape for generic application by connecting a number of standard modular units. The size and shape of the basic modular units are being carefully investigated and determined that meet a mix of requirements, including constructability and ease of marine installation as well as connectivity and flexibility in meeting the global shape and size of the intended land on sea. A key work scope in MMFS is the development of a few types of module connections that feature ease in connection (and disconnection) between modules in marine condition resulting in the desired type of connection rigidity.

This paper presents the development of innovative design concepts for the FHSF and FB. Numerical simulations on the stability, structural and hydrodynamic performance are conducted and results are discussed. Physical model tests have also been performed to validate the proposed design concept for the FHSF. The research work on MMFS is currently ongoing. Owing to the confidentiality of the studies on MMFS, this paper will only cover the study on FHSF and FB.

2 Floating Hydrocarbon Storage Facility

Hydrocarbons are a primary energy source for Singapore. This research track focuses on evaluating existing design concepts, and developing innovative and optimal structural, foundation and construction solutions for a floating hydrocarbon storage facility. The concept developed shall be suitable for hydrocarbon storage at shallow sea depths. Solutions for large sea depths will require substantial different solutions although some generic technology (material technology, linking systems, etc.) may be adaptable also to other locations and conditions. The generic technology developed through the project should also be applicable to other types of structures and locations and have the potential for world-wide use.

The floating fuel storage facility shall meet the following requirements:

   i. The facility shall have a storage capacity of at least 300,000 m^3 of fuel oil and clean petrochemical products (CPP);
  ii. The concept will be aimed at oil storage; gas storage requires substantial different solutions and will not be included;
 iii. Occupation of the sea space shall be optimized;
  iv. The classification rules and safety measures against fire, explosion, oil leakage and collision with small ships shall be satisfied;
   v. The design working life shall be 60 years with minimum maintenance;
  vi. The facility should facilitate loading/offloading operations and blending of fuel mixtures;
 vii. Provision of spaces for Piping/Mechanical/Electrical/Instrumentation (PMEI) system should be allocated in the facility;
viii. The facility must be easily assembled/disassembled so that the facility may be moved elsewhere if required;
  ix. The construction and installation of the facility must be cost-effective;
   x. Future climate change should not affect the safety/serviceability of the facility;
  xi. Existence of the facility shall not disturb/harm the current marine environment;
 xii. The concept shall be applicable or adaptable to other environmental conditions including deep sea;
xiii. Environmental impact—sustainable utilization of raw material.

2.1 Design Concept

The concept for a floating hydrocarbon storage facility may be categorized into six design components, namely the global structural arrangement (see Fig. 1), storage principle (see Fig. 2), positioning and station keeping system (see Fig. 3), storage tank shape (see Fig. 4), tank wall design (see Fig. 5) and tank connections (see Fig. 6). Based on various design choices for each design component, five distinct design concepts have been proposed that suit Singapore coastal water condition.
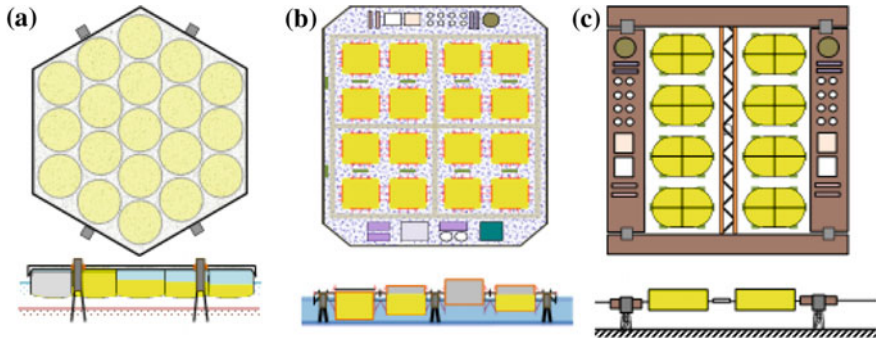
Fig. 1 Global arrangement: **a** monolithic structure, **b** tanks enclosed by platform and **c** tanks enclosed by barges
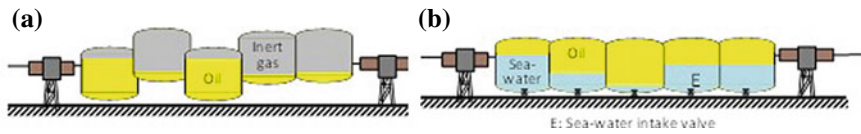

Fig. 2 Storage principle: **a** conventional principle and **b** water displacement principle
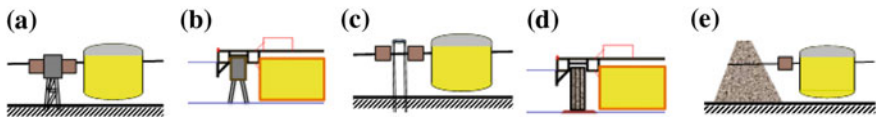

Fig. 3 Positioning and station-keeping: **a** jacket dolphin, **b** jack-up dolphin, **c** mono-pile, **d** sand-filled caisson and **e** sand berm
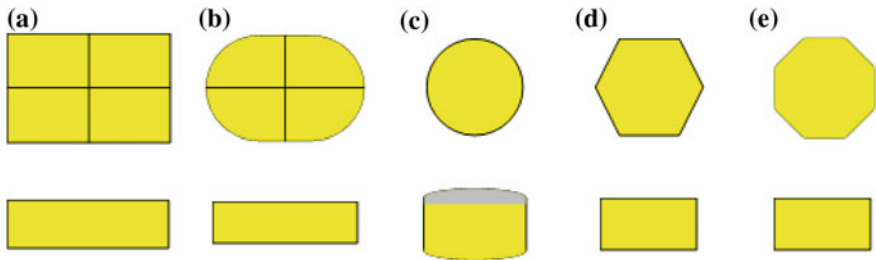

Fig. 4 Storage tank shape: **a** rectangular tank, **b** rectangular tank with rounded corners, **c** cylindrical tank, **d** hexagonal tank and **e** octagonal tank
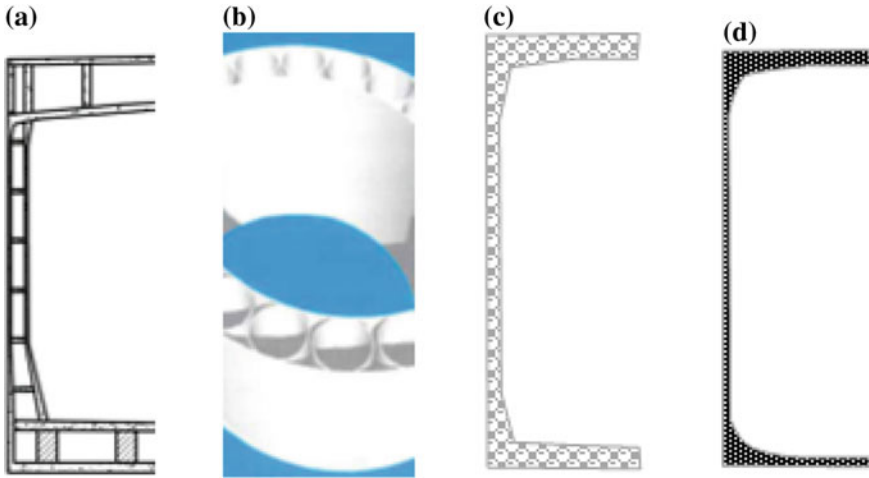
Fig. 5 Tank wall design: **a** double hull wall with horizontal and vertical stiffeners, **b** double hull with vertical stiffeners, **c** lightweight tank wall (lightweight material or wall with voids) and **d** single hull wall
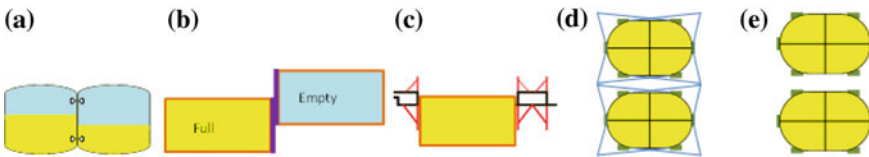

Fig. 6 Tank connection: **a** fixed connection, **b** vertical sliding connection, **c** guide frame connection **d** moored connection and **e** fendered connection

A workshop was organized for the research team to present the proposed design concepts to participants and interact with them to assess these design concepts. The workshop participants included public authorities, universities, research institutions and the offshore and oil industry. From the vibrant discussions between the research team, invited guests and technical advisors, a winning design concept was selected and the team gathered a wide range of valuable feedback from the workshop participants.

Based on the feedbacks from the workshop participants, the research team further improved the selected design concept. Figure 7 shows the conceptual drawings of the proposed FHSF [1]. This concept is self-contained with all essential facilities such as power generation plant, desalination plant, slop and wastewater treatment plant, control room, warehouse, pump rooms, offices and accommodation quarters for workers. It has floating berths on the sides for loading/offloading operations and bunker supply. The floating berths and barges also serve as a protection of the fuel storage modules against waves and ship collision.
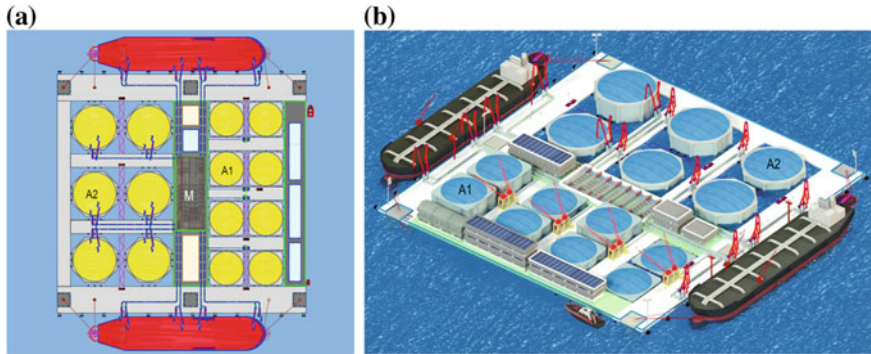
Fig. 7 Floating hydrocarbon storage and bunker facility: **a** plan view and **b** architectural rendering view

The FHSF stores hydrocarbon and provides bunker fuel to ships in harbours. The individual tanks are designed such that they are self-stabilising and the maximum tilt angle under environmental loads does not exceed allowable limits. Depending on the types of product stored, the tanks are categorized into two groups, namely the small tanks and the big tanks. The small tanks are for Clean Petrochemical Products (CPP) and their practical storage capacity ranges from 5000 to about 15,000 m^3 (see A1 in Fig. 1). The big tanks are for crude and fuel oil and they have a practical storage capacity ranging from 20,000 to 35,000 m^3 (see A2 in Fig. 1).

2.2 Stability and Motion Criteria of Floating Tanks

Central to the feasibility of the proposed FHSF is the stability and motion of the storage tanks under environmental loads. The floating hydrocarbon storage tanks must be self-stabilising and the displacements of the tank must not exceed limiting values. The latter is required so that loading and offloading processes are not disrupted during operations and the tank does not capsize or damage the surrounding structures and facilities under extreme weather conditions. Currently, there are no available design codes or standards for the stability design of floating tanks and there are no specifications for the limiting values of tank motion. Thus, the recommended limits for design checks on tanks' stability and motion criteria were proposed based on a critical review of existing design guidelines and philosophy for onshore oil tanks and offshore floating vessels [2]:

i. The initial metacentric height GM of moored tanks shall not be smaller than 0.15 m;
ii. In addition to (i), floating tanks that are fully exposed to the open sea need to fulfill all stability requirements as specified by DNV rules for classification of ships [3];
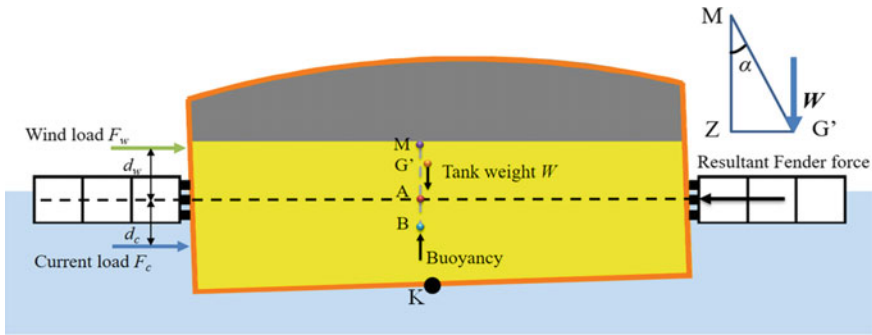
Fig. 8 Floating tank enclosed by barges and subjected to wind and current loads

iii. Rotational (roll/pitch/yaw) motions of moored tanks shall not exceed 2° under working environmental condition;

iv. Sway and surge movements of moored tanks shall not exceed 3 m, and rotational (roll/pitch/yaw) movements of moored floating tanks shall not exceed 5° under extreme environmental condition.

The acceptable limits on the movement of tanks under extreme condition need to be further assessed by detailed hydrostatic and structural analyses results as well as operational considerations. The principle is that these critical movements should not cause damage or loss of integrity and stability to the tank itself and surrounding structures and facilities. Additional motion criteria shall be considered for the construction and installation stage. Furthermore, the freeboard of the tank is assumed to be about 2.5–3 m, which is important to protect the roof structures from direct wave slamming.

Consider a floating hydrocarbon storage tank enclosed by floating barges on the sides. In view of the barges protecting the tanks from incoming waves, we shall assume for the analysis that the tank is mainly subjected to wind and water current loads as shown in Fig. 8. The yellow field in the tank represents the stored hydrocarbon product. The wind and water current speeds are assumed to be constant in the model so that a simple static analysis is possible [4]. In addition, the fenders are designed to restrain the horizontal motion within prescribed limits. Thus, only angular movements, i.e. tilting motion, will be studied.

With the given information on structural configuration and geometry of tank components as well as fuel loading condition, we can estimate the locations of the tank's centre of gravity (CG) and centre of buoyancy (CB) as shown in Fig. 8. The initial metacentric height GM may be calculated from

$$GM = KB + BM - KG \tag{1}$$

where M, G, B and K are the metacentre, the centre of gravity, the centre of buoyancy and the keel, respectively. In a partially filled condition, there will be a shift in liquid
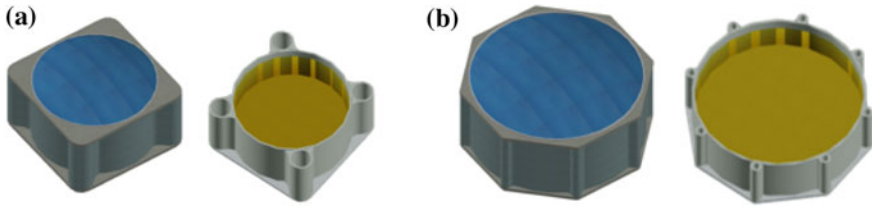
Fig. 9 Storage tanks: **a** small CPP tank and **b** big crude oil tank

Table 1 Geometric and material properties

Parameter	Value
Concrete density	2000 kg/m^3
Seawater density	1025 kg/m^3
CPP density	870 kg/m^3
Crude oil density	1010 kg/m^3
Tank wall thickness	450 mm
Floater wall thickness	350 mm
Roof slab thickness	200 mm
Bottom slab thickness	750 mm

surface given a small tilt on the structure due to the existence of free liquid surface; this is known as Free Surface Effect (FSE) that further reduces the GM, which should be accounted for in the calculation. In addition, the wind and water current loads acting on the structure can be assumed as a uniformly distributed load on the tank wall [5]. The wind and current pressure can be acting in two opposing directions or in the same direction. The maximum case between these two cases that yields the most severe destabilising moment is used for calculations.

The tilting angle of the tank can be calculated based on moment equilibrium about point A, the intersection between resultant fender reaction and the metacentric radius (BM) as shown in Fig. 1. The formula for calculating the tilting angle α is

$$W \times \text{GM} \tan \alpha = |F_w d_w| + |F_c d_c| \tag{2}$$

where W is the weight of the tank, F_w and F_c are the resultant wind load and water current load exerted on the tank walls, d_w and d_c are the lever arms from the centre of the wind load and current load to point A, respectively.

In the FHSF, the tank design features a single hull cylindrical tank with a dome roof on top, a flat slab at the bottom, and several hollow cylindrical floaters attached to the tank wall for both buoyancy and stability, as shown in Fig. 9. This single hull design enjoys nearly balanced hydrostatic pressure on the tank walls. The tank has a diameter D and height H. The dome roof has a common rise to span ratio $Hr/D = 1/8$. Table 1 lists the key properties of the storage tanks. The wind and water current speed at the selected site in Singapore coastal water are listed in Table 2.

Table 2 Wind and current speeds

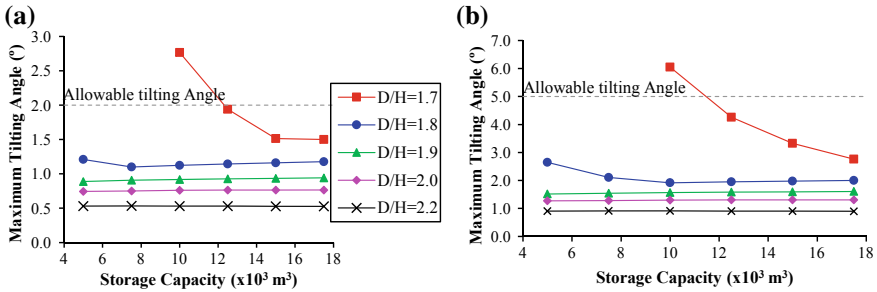| Parameter	Value (m/s)
1-year hourly mean maxima wind speed	15.9
100-year hourly mean maxima wind speed	24.0
1-year hourly mean maxima current speed	1.46
100-year hourly mean maxima current speed	1.90

Fig. 10 Maximum tilting angle of small tanks under **a** 1-year design load and **b** 100-year design load
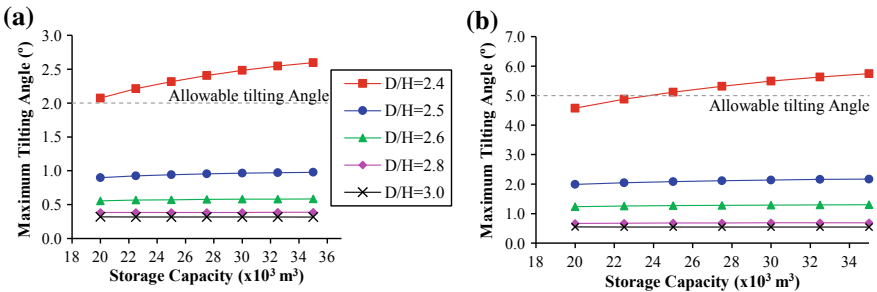

Fig. 11 Maximum tilting angle of big tanks under **a** 1-year design load and **b** 100-year design load

Figure 10 presents the maximum tilting angles of small CPP storage tanks of various storage capacities under wind and current loads at their 1-year and 100-year return periods. It is clear from the figure that larger tank D/H ratios lead to smaller tilting angles (and thus the tanks are more stable). Results show that tanks with $D/H = 1.7$ fulfil the stability and operational requirements on tilting motion when the storage capacity is above 12,500 m^3. When tank D/H reaches 1.8, all the considered tanks satisfy the aforementioned design checks. Similarly, the maximum tilting angles of big oil storage tanks under wind and current loads are presented in Fig. 11. As it can be seen, a D/H ratio exceeding 2.4 is necessary for oil storage tanks to satisfy stability and tilt motion criteria.

2.3   *Structural and Hydrodynamic Analyses*

Besides the study on hydrostatic stability and quasi-static motion of floating tanks, detailed finite element analysis of the storage tank structure [6] was conducted. Analysis results show that it is possible to avoid the need for vertical prestressing tendons with the introduction of a tapered tank wall at the tank bottom.

Comprehensive hydrodynamic analyses of floating tanks considering fender connection to the surrounding barges [7] and compliant tether mooring lines [8] were carried out. Hydroelastic response analysis of the surrounding barges was also investigated [9]. Detailed model tests on single floating tanks [10], multiple floating tanks and the entire floating facility were conducted. Results show that the hydrodynamic performance of the tanks and barges is satisfactory even with environmental conditions corresponding to a 100-year return period, thereby validating the proposed conceptual design for deployment in Singapore coastal waters.

3   Floating Bridge

Bridges are essential in connecting islands and land parcels separated by a water body to boost economic and leisure activities. When water is very deep and/or the seabed is extremely soft at a location where a bridge is going to be built, conventional piers supporting the bridge become expensive or even impractical. Under these conditions, floating bridges may offer distinct advantages through the use of pontoons to support the bridge deck. The pontoons are supported by natural buoyancy forces and are not dependent on the sea bed condition. More importantly, if the bridge is to be relocated elsewhere when it is no longer needed, a floating bridge allows easy removal as it may be towed away by tug boats.

The second track of MPFS project focuses on evaluating existing design concepts and developing innovative structural, foundation and construction solutions for a floating bridge spanning across waterbodies. The design of the FB should be suitable for shallow water depths and accommodate daily tidal variations at the site which is just next to the Marina Barrage. The design concept shall meet the following requirements:

  i. The bridge must have sufficient clearance; at least 15 m over the water surface and clear span for maintenance vessels, commercial river taxis and ad-hoc boats during special events to pass underneath;
 ii. The water flow discharged from Marina Barrage (current speed up to 1.5 m/s) shall not endanger the serviceability of the bridge;
iii. The total length of the bridge will be approximately 500 m;
 iv. The width of the bridge must be at least 38.6 m in order to accommodate 3 lanes of traffic in both directions;
  v. The design service life shall be 100 years with minimum maintenance;
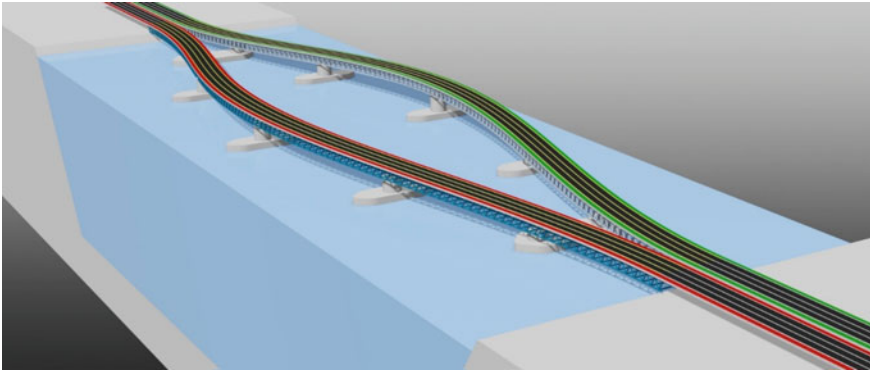 vi. The construction and installation of the bridge must be cost-effective;

Fig. 12 Aerial view of floating double lateral curved bridge

  vii. The bridge design should cater for efficient construction, assembly and decommissioning;

 viii. Future climate change should not affect the safety/serviceability of the bridge;

   ix. The bridge shall have minimal environmental impact and shall not harm current marine environment;

    x. Sustainable utilization of raw material shall be considered;

   xi. The bridge should be aesthetically attractive and design should be adapted to the surrounding environment.

3.1 Design Concept

Based on the design requirements specified above, a concept entitled "floating double lateral curved bridge", as shown in Fig. 12, was proposed by the research team. This design concept comprises two oppositely curved pontoon bridges, each carrying a 3-lane roadway and a pedestrian walkway. The bridges are supported by several pontoons spaced at 100–120 m apart. The double arch bridge structures hug an elliptical sea space which may be used to house a suitable structure.

An arch is a much stronger member than a straight beam when subjected to in-plane loadings as it transfers the loadings in axial rather than in bending and shear as in the case of a straight beam. Additionally, an arch will provide more torsional rigidity which improves the resistance to the rolling motion. The double lateral curved bridge achieves not only an aesthetic design but also forms an effective structural system. Hence, the laterally curved configuration is adopted for the bridge deck in order to achieve a mooring free bridge with a clear span across the water body.

However, a drawback of using a laterally curved configuration is the increased reaction at the supports. Figure 13 shows the free body diagrams of a (a) straight beam and (b) simply supported arch that are subjected to an in-plane point load at the
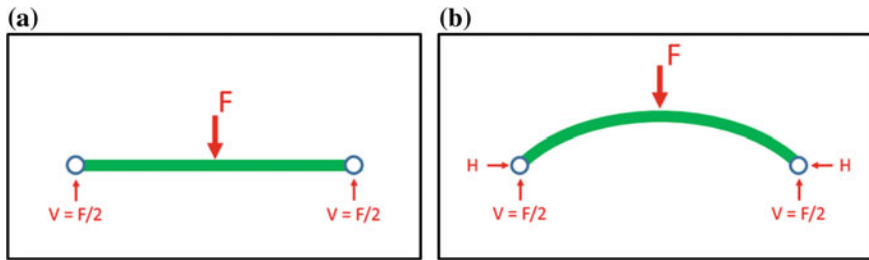
Fig. 13 Free body diagram of **a** straight beam and **b** curved beam

midspan. Clearly, the end reactions of an arch will always be greater than a straight beam due to the existence of horizontal force components. Note that the magnitude of the horizontal reaction component depends on the curvature, stiffness, and opening angle of the arch. According to the practical experience, such a horizontal reaction can be larger than the vertical reaction component in many real-life cases. Thus, a curved bridge will usually require a stronger bridge end support. To overcome this complication, the double curved bridge is proposed to cancel out the undesirable horizontal force components at the points where two bridges join. Figure 14 shows the schematic force diagram of a double lateral curved bridge subject to current and wind loads. As illustrated in Fig. 14, the environmental loads will put one bridge in compression through arch effect and the other in tension via catenary effect. It is expected that the forces will generally be in the same order of magnitude. Consequently, the sum of the horizontal reaction component experienced at the intersections of the two curved bridges is expected to be small. It is thus innovative to adopt a double curved configuration due to the force cancellation effect; thereby resulting in the curved bridge to be similar to a straight bridge as far as support reaction is concerned.

The coastal areas are subject to daily tidal variations that must be accounted for in the design of bridges. The tidal variations impose challenges to the design of bridge abutment and the connection for the floating bridges as the bridge structures are floating up and down with the tides. In the current design proposal, the bridge structure stiffness is specially designed so that the bridge is able to deform with the tidal changes (see Fig. 15).

In summary, the proposed floating bridge design has the following key features:

i. The pontoons are designed to support through buoyancy the self-weight of the bridge as well as the vehicle load.
ii. The double lateral arch bridge floats stably on water.
iii. The overall bridge design ensures that there are minimal lateral motions owing to the arch and catenary effects and hence no moorings are required to hold the pontoons in position.
iv. The curvature of the arch bridge is designed optimally to meet design and operational requirements.
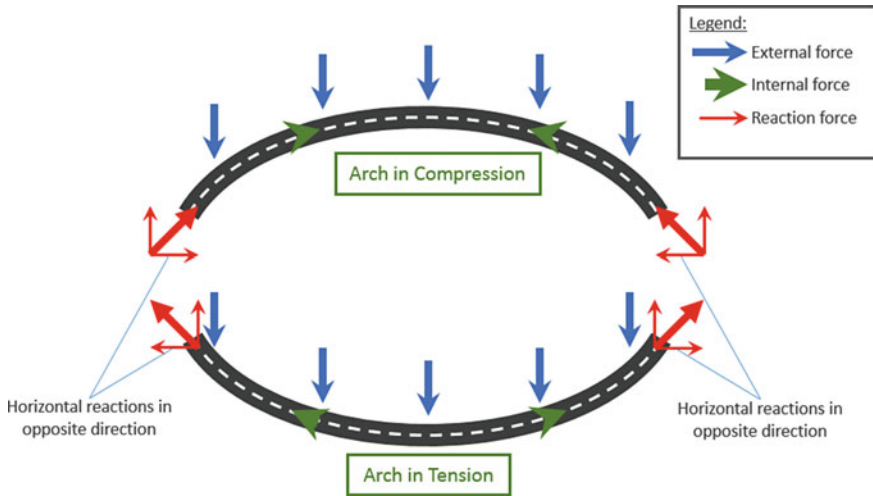v. The bridge can be designed to have the flexural rigidity to adapt to the tidal variations.

Fig. 14 Force diagram of double lateral curved bridge

Fig. 15 Principle of bridge to adapt tidal variations

vi. Double-curved geometry is adopted with the intention to cancel the axial reaction force component at the point of intersection of the two curved bridges.

vii. The bridge is modular in design and can be prefabricated in parts offsite to minimize the onsite construction efforts and the impact on the local environment.

3.2 Analytical Study for Single Curved Floating Bridge

It is essential to understand the mechanisms corresponding to a floating curved bridge adapted to the daily tidal variations. In addition, the generally soft soil condition in Singapore coastal waters also have implications for the load carrying mechanism and structural performance of the curved bridge. In order to get insights into the physical behavior of the bridge structure, an analytical solution to the responses of a curved bridge in and out of the curvature plane was developed.

Figure 16 shows a beam model of the curved bridge. The bridge has a radius of curvature R and an overall length L. The angle subtended at the centre of curvature is θ. In the global Y-direction, the beam is discretely supported by pontoons, which
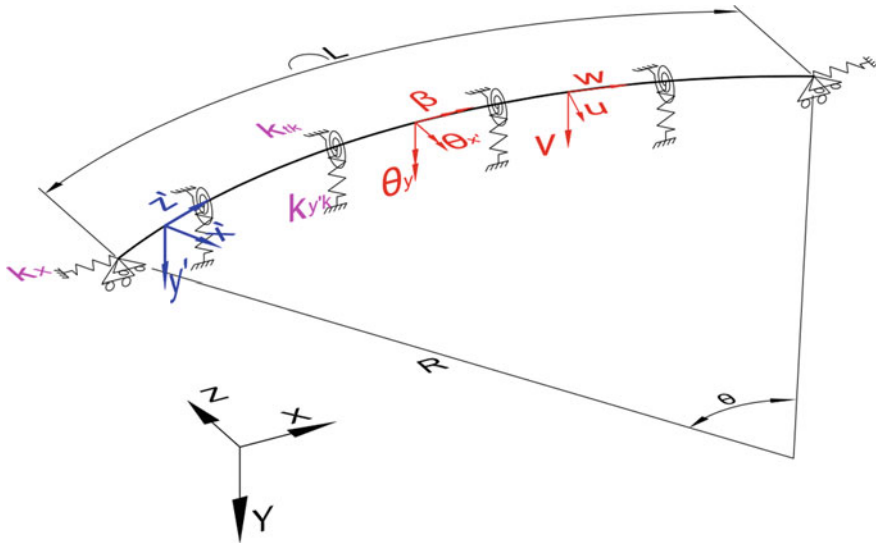
Fig. 16 Coordinates system and boundary conditions of curved beam

are modelled as linear and torsional springs of stiffness $k_{y'k}$ and k_{tk}, respectively. Additionally, translational and torsional restraints are imposed at the ends of the bridge to prevent the beam from displacing in global Y-direction as well as rotating about its local z' axis. In the global X-direction, linear springs, $k_{s,X}$ are added at both ends to represent the effect of soft soil foundation. Similar boundary conditions should also be applied to the beam in the global Z-direction. However, the beam is assumed to be simply supported at two ends instead. This is because the reaction forces in Z-direction are always statically determinate and have no effect on the internal forces. Therefore, it is reasonable to adopt this simplification. The movement of the abutment in the global Z-direction is a rigid body motion which can be easily computed once the foundation stiffness is known. According to the classical theory [11], the in-plane responses of a curved beam are decoupled from its out-of-plane responses. Hence, the solutions to the in-plane and out-of-plane responses can be derived independently.

In the curvature plane, the bridge is subject to wave and current forces acting on the pontoons. The spring deformations representing the soft soil foundation restraint at the bridge ends are denoted as δ_H. According to Young and Budynas [12], the horizontal displacement of the end support may be assumed to be caused by (a) a vertical concentrated force along the beam or (b) a horizontal concentrated load acting at roller end as shown in Fig. 17a, b, respectively. The horizontal deformation at beam end for case (a) is given by [12]
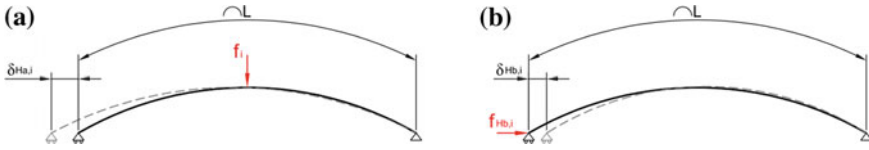
$$\delta_{Ha,i} = -\frac{R^3}{EI_{y'}}(LP_{Ha}) \tag{3}$$

Fig. 17 Pin-roller supported arch subject to **a** vertical and **b** horizontal point loads

where LP_{Ha} is the loading terms which takes into account the geometry and properties of the beam, as well as the location and magnitude of the applied load, which may be expressed as

$$
LP_{Ha} =
$$
$$
f_i \left[\frac{\theta}{2}\sin\frac{\theta}{2}\cos\frac{\theta}{2} - \text{Ø}\sin\text{Ø}\cos\frac{\theta}{2} + \frac{k_1}{2}\left(\cos^2\frac{\theta}{2} - \cos^2\text{Ø}\right) + k_2\cos\frac{\theta}{2}\left(\cos\frac{\theta}{2} - \cos\text{Ø}\right) \right] \tag{4}
$$

where f_i is the ith external transverse load applied to the bridge; θ and ϕ are the subtended angle of the curved beam and the angle measured counter-clockwise from the mid-span of the beam to the position of load, respectively; and k_1 and k_2 are the correction factors for shear and hoop stress, respectively. Similarly, for case (b), the displacement of the roller support can be computed from

$$
\delta_{Hb,i} = -\frac{R^3}{EI_{y'}}(LP_{Ha}) \tag{5a}
$$

$$
LP_{Hb} = f_{Hb,i}\left[\theta\cos^2\frac{\theta}{2} + \frac{k_1}{2}(\theta - \sin\theta) - k_2\sin\theta \right] \tag{5b}
$$

It is clear from Eq. (5b) that $f_{Hb,i}$ can be used to represent the reaction force of a spring shown in Fig. 16. A strain compatibility relationship can be employed to obtain the actual spring deformation due to the ith external transverse load. By setting up the equilibrium state of the curved beam, the internal member forces can be directly evaluated.

Unlike the support condition of the curved beam for the in-plane case, the beam is discretely supported at the locations of the pontoons owing to the buoyancy out of the curvature plane, as shown in Fig. 16. By neglecting the inertia and viscous damping terms, the out-of-plane governing equations may be written as [11]

$$
\frac{\partial^2}{\partial z^2}\left(EI_x(z)\frac{\partial^2 v}{\partial z^2} - \frac{1}{R}\beta \right) - \frac{GJ(z)}{R}\left(\frac{1}{R}\frac{\partial^2 v}{\partial z^2} + \frac{\partial^2\beta}{\partial z^2} \right)
$$
$$
+ \sum_{k=1}^{Np} k_{yk}(v - H_T - H_e)\delta(z - z_k) = \rho A(z)g \tag{6a}
$$

$$\frac{EI(z)}{R}\left(\frac{\beta}{R}-\frac{\partial^2 v}{\partial z^2}\right)-GJ(z)\left(\frac{\partial^2 \beta}{\partial z^2}+\frac{1}{R}\frac{\partial^2 v}{\partial z^2}\right)+\sum_{k=1}^{Np}k_{tk}\beta\delta(z-z_k)=0 \quad (6b)$$

where v and β are the vertical displacement and torsional deformation, respectively; k_{yk} and k_{tk} the vertical and torsional hydrostatic stiffness, respectively; Np refers to the number of pontoons; H_T and H_e are the tide-induced surface elevation and the water surface elevation in the equilibrium state.

In view of the boundary conditions and the relationship between v and β, both vertical and torsional deformations of the curved beam can be expressed as the summation of a series of sinusoidal functions as

$$v=\sum_{i=1}^{n}q_{vi}\sin\frac{i\pi z}{L},\ \beta=\sum_{i=1}^{n}q_{\beta i}\sin\frac{i\pi z}{L} \quad (7)$$

where q_{vi} and $q_{\beta i}$ denote the generalized coordinates of the ith mode; and n the number of modes. To solve the coupled differential equations, Galerkin's approach is adopted to formulate the weighted residual forms of the governing equations, which leads to ith mode governing equations

$$\sum_{j=1}^{n}a_{ij}q_{vj}+\sum_{j=1}^{n}b_{ij}q_{\beta j}=\rho g\int_0^L A(z)\sin\left(\frac{i\pi z}{L}\right)dz \quad (8a)$$

$$\sum_{j=1}^{n}c_{ij}q_{\beta j}+\sum_{j=1}^{n}d_{ij}q_{vj}=0 \quad (8b)$$

where the coefficients are given by

$$a_{ij}=\int_0^L\left[EI_x(z)\left(\frac{i\pi}{L}\right)^4+\frac{GJ(z)}{R^2}\left(\frac{i\pi}{L}\right)^2\right]\sin\left(\frac{i\pi z}{L}\right)\sin\left(\frac{j\pi z}{L}\right)dz$$
$$+\sum_{k=1}^{Np}k_{yk}\sin\left(\frac{i\pi z_k}{L}\right)\sin\left(\frac{j\pi z_k}{L}\right) \quad (9a)$$

$$b_{ij}=\frac{1}{R}\left(\frac{i\pi}{L}\right)^2\int_0^L(EI_x(z)+GJ(z))\sin\left(\frac{i\pi z}{L}\right)\sin\left(\frac{j\pi z}{L}\right)dz \quad (9b)$$

$$c_{ij}=\int_0^L\left[\frac{EI_x(z)}{R^2}+GJ(z)\left(\frac{i\pi}{L}\right)^2\right]\sin\left(\frac{i\pi z}{L}\right)\sin\left(\frac{j\pi z}{L}\right)dz$$
$$+\sum_{k=1}^{Np}k_{tk}\sin\left(\frac{i\pi z_k}{L}\right)\sin\left(\frac{j\pi z_k}{L}\right) \quad (9c)$$

$$d_{ij}=\frac{1}{R}\left(\frac{i\pi}{L}\right)^2\int_0^L(EI_x(z)+GJ(z))\sin\left(\frac{i\pi z}{L}\right)\sin\left(\frac{j\pi z}{L}\right)dz \quad (9d)$$
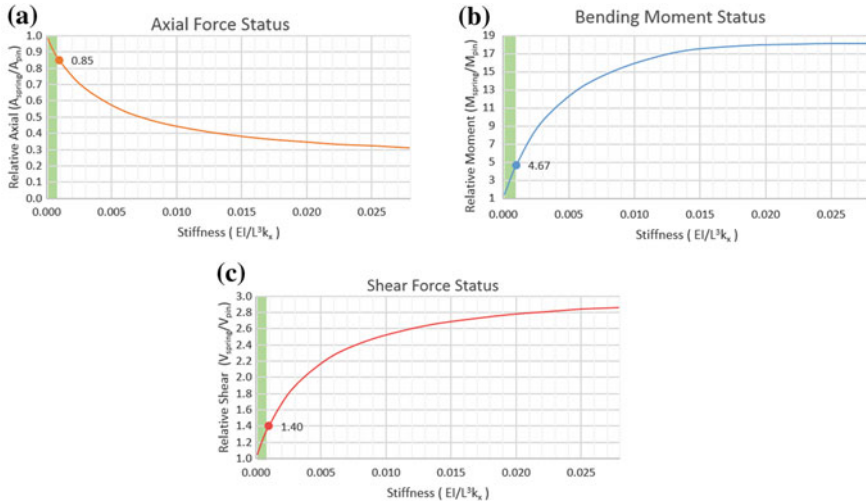
Fig. 18 Bridge in-plane response

The accuracy and computational efficiency of the analytical solutions have been documented in the authors' earlier publications [11, 13]. To study the effect of soft soil foundation on the in-plane response of a curved floating bridge, a numerical investigation was carried out by conducting a series of parametric studies with different stiffness ratios of the bridge's flexural rigidity, $EI_{y'}/L^3$ to the foundation stiffness at bridge ends, k_x. Figure 18 presents the ratio of the forces in a spring supported curved bridge to those of a pin supported curved bridge. Different bridge structural stiffness to soft soil foundation stiffness ratios are considered. It can be seen that for this particular load arrangement, the reduction in the axial force can be up to 70% which in turn amplifies the bending moment by 18 times as the foundation stiffness reduces. Hence, it is crucial that a sufficient rigidity of the end abutment is retained so as to ensure that the membrane action of the curved bridge is effectively activated. For example, at least 85% of the axial force accompanied by 367% increment in the bending moment can be achieved by a stiffness ratio EI/L^3k_x smaller than 1×10^{-4}.

The effect of tide-induced water surface elevation is next investigated. Figure 19 shows the vertical displacement and torsional deformation of the bridge when it is subjected to a 2 m low tide. Note that the range of the out-of-plane stiffness of the curved bridge is practically selected based on the sectional properties of the Norwegian Bergsøysund bridge. It is observed from Fig. 19 that the vertical displacement and rotation angle of the bridge start to converge when the out-of-plane second moment of inertia exceeds 10 m⁴. When the bridge stiffness is too low, i.e. $I_x = 1$ m⁴, the bridge spans between two adjacent pontoons exhibit noticeable deflections due to the self-weight of the bridge. Such magnitude is definitely not acceptable as it will not only hinder the serviceability of the bridge but it may also lead to rupture of the superstructure and the bridge deck. On the other hand, if the bridge stiffness
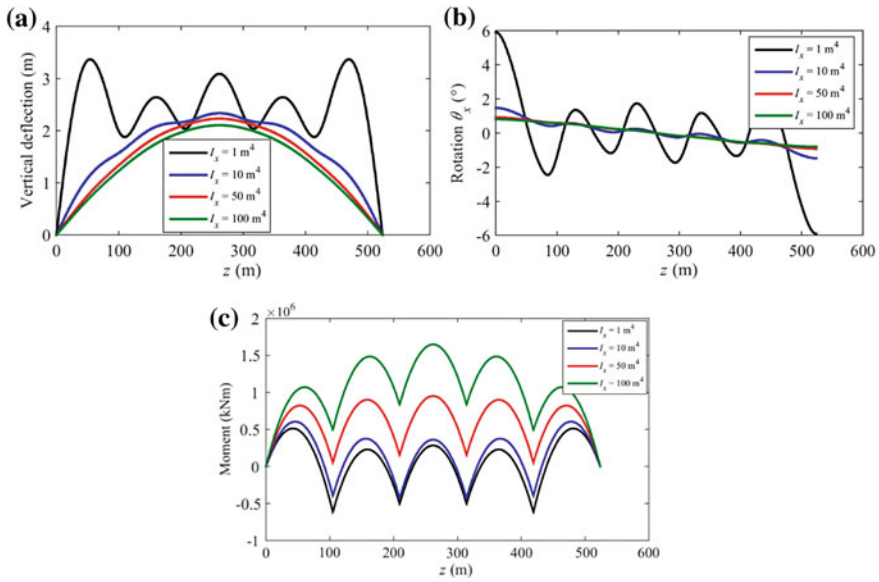
Fig. 19 Curved bridges with different flexural rigidities subject to tidal variations
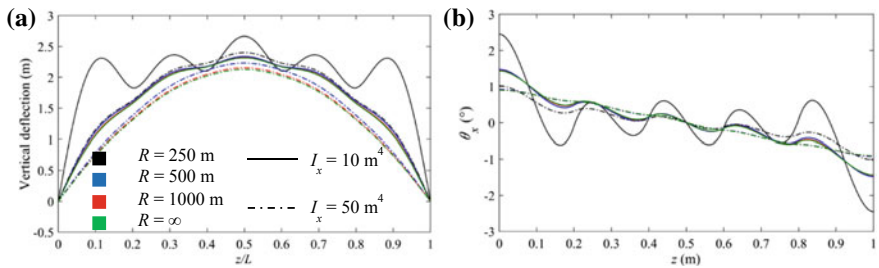

Fig. 20 Curved bridges with different radii and flexural rigidities subject to tidal variations

is too large, i.e. $I_x = 100$ m^4, the bridge will be subject to huge bending moments although the deflection is restrained. In view of Fig. 19, it may be reasonable to design a bridge with an out-of-plane second moment of inertia in the range of 10–50 m^4 which results in a well-restrained deflection under high/low tides and does not attract large bending moment acting on the bridge.

Figure 20 shows the effect of both structure stiffness and radius on the out-of-plane responses of the curved bridge under a 2 m tide. As it can be seen, when the radius of the bridge is small, the vertical displacement is large. This is due to the fact that the bridge span is also large. However, when the radius exceeds 500 m, the effect of the bridge radius is found to be small. When this is read in conjunction with the in-plane responses of a curved bridge, one may conclude that the optimum bridge radius ranges from 500 to 1000 m.

3.3 Hydrodynamic Study of Double Curved Floating Bridge

Section 3.2 is concerned with a static analytical study of a single curved bridge. In order to investigate the dynamic response of a double lateral arch bridge and the effect of force cancellation at the bridge ends, a more detailed numerical model was constructed. In the numerical model, the bridge structure is modeled as flexible beams supported by elliptical cylindrical pontoons that float on water surface. Parametric study of the bridge structural rigidity was performed to investigate its effect on the structural and hydrodynamic responses. White noise, regular and irregular wave simulations were carried out in the numerical investigation. The analysis results demonstrate that the floating bridge concept is valid when the structural rigidity is well chosen. For more details, one may refer to the published results in [14].

4 Conclusions

This paper presents the development of innovative design concepts for a floating hydrocarbon storage facility (FHSF) and a floating bridge (FB). Numerical simulations on the stability, structural and hydrodynamic performances were conducted. The results show that constructing large floating structures in Singapore coastal waters is very doable owing to the benign sea state. Besides FHSF and FB, other potential applications for VLFS include floating LNG regasification facilities, desalination plants, piers and even towns or cities.

References

1. Wang, C. M., Ang. K. K., Dai, J., Lim, B. K., Magee, A. R., & Watn, A, et al. (2017). *Floating Hydrocarbon Storage and Bunker Facility*. Singapore Provisional Patent 10201702591X.
2. Ang. K. K., Dai, J., Lim, B. K., & Wang, C. M. (2017). Floating hydrocarbon storage and bunker facility. In *Proceedings of the 10th International Research Conference of KDU*. Ratmalana, Sri Lanka, 3–4 Aug 2017.
3. DNV. (1995). *Rules for classification of ships*. Part 3 Chapter 4: Stability and watertight integrity. Norway: Det Norske Veritas.
4. DNV. (2011). *DNV-OS-C301: Stability and watertight integrity*. Norway: Det Norske Veritas.
5. DNV. (2010). *DNV-RP-C205: Environmental conditions and environmental loads*. Norway: Det Norske Veritas.

6. Jiang, D., Tan, K. H., Dai, J., Ong, K. C. G., & Heng, S. (2018). Structural performance evaluation of innovative prestressed concrete floating fuel storage tanks. *Structural Concrete, 20,* 15–31. https://doi.org/10.1002/suco.201800032.

7. Wan, L., Han, M., Jin, J., Zhang, C., Magee, A. R., Hellan, O., et al. (2018). Global dynamic response analysis of oil storage tank in finite water depth: Focusing on fender mooring system parameter design. *Ocean Engineering, 148,* 247–262.

8. Wan, L., Zhang, C., Magee, A. R., Jin, J., Han, M., Ang, K. K., et al. (2018). An innovative mooring system for floating storage tanks and stochastic dynamic response analysis. *Ocean Engineering, 170,* 361–373.

9. Dai, J., Ang, K. K., & Zhang, C. (2019). Hydroelastic analysis of modular floating barges for hydrocarbon storage facility. In *Proceedings of the 1st Vietnam Symposium on Advances in Offshore Engineering*, Hanoi, Vietnam, 1–3 Nov 2018.

10. Zhang, C., Dai, J., Ang., K. K., & Magee, A. R. (2019). Comparison study on bottom plate effect on single hydrocarbon storage tank through decay test. In *Proceedings of the 1st Vietnam Symposium on Advances in Offshore Engineering*, Hanoi, Vietnam, 1–3 Nov 2018.

11. Dai, J., & Ang, K. K. (2015). Steady-state response of a curved beam on a viscously damped foundation subjected to a sequence of moving loads. *Proceedings of the Institution of Mechanical Engineers, Part F: Journal of Rail and Rapid Transit, 229,* 391–442.

12. Young, W. C., & Budynas, R. G. (2002). *Roark's formulas for stress and strain* (7th ed.). Darby, USA: McGraw-Hill.

13. Dai, J., Ang, K. K., & Lim, B. K. (2017). Response of a floating curved pontoon bridge subjected to tide induced water surface variation: an analytical approach. In *Proceedings of the 10th International Research Conference of KDU*. Ratmalana, Sri Lanka, 3–4 Aug 2017.

14. Wan, L., Magee, A. R., Hellan, O., Watn, A., Ang, K. K., & Wang, C.M. (2017). Initial design of a double curved floating bridge and global hydrodynamic responses under environmental conditions. In *Proceedings of the 36th International Conference on Ocean, Offshore & Arctic Engineering*. Trondheim, Norway, 35–30 June 2017.